Original Research *Highlight article*

Tastin promotes non-small-cell lung cancer progression through the ErbB4, PI3K/AKT, and ERK1/2 pathways

Andong Yue[1]*, Maoxi Chen[1,2]*, Shihui Dai[1], Yiyin Zhang[1], Wei Wei[1], Lulu Fan[1], Fang Wang[1], Fei Zhang[1], Hanqing Yu[1], Yan Lu[3] and Yu Lei[1]

[1]Department of Oncology, The First Affiliated Hospital of Anhui Medical University, Hefei 230022, P.R. China; [2]Department of Oncology, Anhui Chest Hospital, Hefei 230022, P.R. China; [3]Department of Gastroenterology, The Second Affiliated Hospital of Anhui Medical University, Hefei 230601, P.R. China
*These authors contributed equally to this paper.
Corresponding author: Yu Lei. Email: leiyu@ahmu.edu.cn

Impact Statement

Anticancer drugs have been developed rapidly in recent years, and agents targeting driver genes have shown great efficacy in treating specific types of lung cancer. Still, acquired drug resistance occurs and affects non-small-cell lung cancer (NSCLC) prognosis. Reliable molecular therapeutic targets are urgently needed in lung cancer. Tastin has been reported to be overexpressed in cancer, but related data in lung cancer are unavailable. This study suggests that tastin expression is elevated in NSCLC and is correlated with a poorer prognosis. The results also showed tastin participates in NSCLC growth and invasion and might be a potential therapeutic target in NSCLC. Hence, tastin might be used as a potential biomarker of NSCLC progression. These data highlight tastin's role in NSCLC occurrence and progression and provide a potential target for the development of new treatments for NSCLC.

Abstract

Tastin might be involved in tumorigenesis, but its role in non-small-cell lung cancer (NSCLC) has not been adequately explored. This work aimed to examine tastin's role in NSCLC and to explore the underlying mechanism. The Gene Expression Omnibus (GEO), Gene Expression Database of Normal and Tumor tissues (GENT), and Cancer Genome Atlas (TCGA) databases were used. Four GEO datasets (GSE81089, GSE40419, GSE74706, and GSE19188) containing gene expression data for NSCLC and normal tissue samples were analyzed for tastin mRNA expression. Tastin expression levels in different tissues were compared using the GENT website. TCGA biolinks were used to download gene expression quantification ($n=594$) and overall survival data ($n=535$). In total, 30 lung adenocarcinoma and 25 lung squamous cell carcinoma cases were enrolled. In addition, four-week-old male BALB/c nude mice ($n=9$/group) were used to establish xenograft mouse models. Furthermore, cultured HEK293T, A549, and NCI-H226 cells assessed. Immunoblot, hematoxylin and eosin (H&E) staining, immunohistochemistry, real-time quantitative reverse transcription polymerase chain reaction (qRT-PCR), fluorescence microscopy, flow cytometry, lentiviral transduction, and MTT, colony formation, wound healing, and Transwell assays were carried out. Tastin expression levels were markedly increased in NSCLC tumor tissue specimens and correlated with a poorer prognosis. Silencing of tastin inhibited the proliferative and migratory abilities of NSCLC cells. Bioinformatic analysis suggested that tastin interacts with ErbB4. The PI3K/AKT and ERK1/2 downstream pathways were suppressed in tastin-deficient cells. In conclusion, tastin might be involved in NSCLC growth and invasion and is a potential therapeutic target in NSCLC.

Keywords: Tastin, non-small-cell lung cancer, ErbB4, PI3K/AKT, ERK1/2

Experimental Biology and Medicine **2023; 248: 519–531. DOI: 10.1177/15353702221147566**

Introduction

In lung adenocarcinoma, non-small-cell lung cancer (NSCLC)-driver genes, such as epidermal growth factor receptor (EGFR), mutant Kirsten rat sarcoma virus (KRAS), and EML4-ALK, are critical driving forces of tumor progression. The most common abnormal genes in lung squamous cell carcinoma are amplified FGFR1 and PI3KCA.[1] Anticancer drugs have been developed rapidly in recent years, and drugs targeting those driver genes (e.g. gefitinib, erlotinib, and crizotinib) are remarkably effective against specific types of lung cancer.[2,3] Nevertheless, acquired drug resistance can occur and severely threaten NSCLC prognosis. Therefore, novel reliable molecular therapeutic targets are particularly urgent in lung cancer.

The *tastin* (also known as *trophinin-associated protein*, *TROAP*) gene encodes a proline-rich protein found in the cytoplasm.[4] When tastin and trophinin (TRO) are co-transfected, trophoblast cells gain the ability to adhere to endometrial cells.[5] Their expression patterns are consistent

with embryo implantation, suggesting that they may induce embryonic cell proliferation and trophoblast cell invasion of the endometrium.[6] Tastin forms a complex with TRO and bystin, participates in adhesion between trophoblast cells and endometrial cells, and mediates early embryo implantation.[7] However, only a few studies have reported the abundance of tastin in tumor tissues.[8–10] Microarray analysis indicated markedly elevated *tastin* gene expression in prostate cancer tissues compared with adjacent tissues, suggesting an important role in tumorigenesis for tastin, which could be considered a prostate cancer-related antigen.[11,12] Tastin participates in the progression of prostate cancer.[13] It also drives hepatocellular carcinoma progression[14] and is associated with its prognosis.[4,15] Nevertheless, the function and underlying mechanisms of tastin in NSCLC have not been adequately investigated. Modulating tastin expression in gastric carcinoma could decrease cancer cell proliferation, migration, and invasion.[16]

Tastin's function in embryo implantation is related to ErbB4 activation.[17] ErbB4 (HER4) belongs to the EGFR family and is considered to participate in tumorigenesis.[18] The expression of ErbB4 is increased in breast, ovarian, and lung cancers.[18,19] Under normal physiological conditions, the extracellular domain of ErbB4 is activated after binding to its ligand. The receptor dimerizes and autophosphorylates, activating downstream pathways, including Ras/Raf/MEK/ERK and PI3K/AKT, which regulate cell differentiation, proliferation, cycle, and apoptosis.[20,21] In patients with NSCLC, ErbB4 overexpression leads to early metastasis and reduced response to chemotherapy.[22] Moreover, the survival rate of patients with NSCLC and ErbB4 overexpression is significantly reduced.[18] A missense mutation in the *ErbB4* gene was reported in NSCLC,[23] which increases the autophosphorylation activity of ErbB4, resulting in ligand-independent activation, promoting the malignant transformation of normal cells and tumor cell proliferation.[18]

Therefore, tastin may be important in tumorigenesis, which may provide a basis for developing a new and effective treatment option for NSCLC. Therefore, this study analyzed multiple public databases and clinical NSCLC samples to determine tastin's role in NSCLC and explore the underpinning mechanism.

Materials and methods

Gene Expression Omnibus database

Four Gene Expression Omnibus (GEO) datasets (GSE81089, GSE40419, GSE74706, and GSE19188) were downloaded (https://www.ncbi.nlm.nih.gov/geo/) with GEO query, as described previously.[24] They included gene expression profiles for NSCLC and non-cancerous tissue specimens, and were selected to analyze the relative tastin mRNA expression levels.

Gene Expression Database of Normal and Tumor tissues database

The U133Plus2 chip type was selected for statistical analysis. The expression of Tastin in different tissues was compared using the GENT database (http://medical-genome.kribb.re.kr/GENT/overview.php).

TCGA

To download gene expression quantification ($n = 594$) and overall survival data ($n = 535$) from the Genomic Data Commons portal (https://portal.gdc.cancer.gov/) and the Lung Adenocarcinoma (LUAD) cohort from the Cancer Genome Atlas (TCGA), a R/Bioconductor package called TCGAbiolinks[25] was used. The Kaplan–Meier (KM) method was used for comparing overall survival in TCGA-LUAD between high- and low-tastin expression cases.

Cell culture

HEK293T, A549, and NCI-H226 cells were cultured in Dulbecco's Modified Eagle Medium (DMEM) containing 10% fetal bovine serum, sodium pyruvate (1 mM), and streptomycin (100 mg/mL), from Gibco.

Western blot

Western blot was performed routinely (Supplementary Material). Primary antibodies targeted tastin (1:500), ErbB4 (1:1000), p-ErbB4 (1:1000), ERK (1:1000), p-ERK (1:1000), AKT (1:1000), p-AKT (1:1000), E-Cadherin (1:1000), and GAPDH (1:1000) were provided by Santa Cruz Biotechnology; those raised against N-Cadherin (1:1000) and Vimentin (1:1000) were from Cell Signaling Technology. The bands were quantified with the ImageJ software.

Immunohistochemistry

Immunohistochemistry was performed to detect tastin and Ki67 in specimens from paraffin sections (Supplementary Material). The primary antibodies were antihuman tastin and anti-Ki67 polyclonal antibodies (Novus Biologicals USA).

Real-time quantitative reverse transcription polymerase chain reaction

Real-time quantitative reverse transcription polymerase chain reaction (qRT-PCR) was carried out routinely (Supplementary Material). Primers were GAPDH, forward 5′-TGACTTCAACAGCGACACCCA-3′ and reverse 5′-CACCCTGTTGCTGTAGCCAAA-3′; tastin, forward 5′-TGCAGAAAACCACCGCTCAATA-3′ and reverse 5′-CCACCAATCTTTGTGATGTCTCT-3′. The $2^{-\Delta\Delta Ct}$ method was used for quantitation.

siRNA

According to the Primer Premier 5.0 software, a sequence was selected as an siRNA sequence for the Tastin gene: CCCGGCAAGCCACGAAGGATC. The siRNAs were purchased from TsingKe BioTech (China).

Packaging, purification, and transfection of lentiviruses

The construction of the employed vectors is described in the Supplementary Material.

Celigo automatic cell counting analyzer

The constructed recombinant plasmid contains the green fluorescence reporter gene (GFP). A Celigo automatic cell counting analyzer (Nexcelom) was used to capture and record fluorescent signals and assess the number of fluorescent cells that reflected cell growth. Cells in the shCtrl (empty vector) and shTastin (tastin-linked shRNA) groups were collected 72 h after infection with lentiviruses. Afterward, 2×10^4 cells/mL were seeded on 96-well culture plates, with 100 μL/well. Then, green fluorescence signals in each well were detected at 24, 48, 72, 96, and 120 h.

MTT assay

Cells in the shCtrl and shTastin groups were collected 72 h after infection with lentiviruses. The MTT assay was performed routinely (Supplementary Material).

Colony formation assay

Cells in the shCtrl and shTastin groups were collected 72 h after infection with lentiviruses. A single-cell suspension (3×10^3 cells/mL) was seeded in 6-well culture plates at 100 μL/well, with medium replacement at three-day intervals. Following a 7- to 10-day culture, fixation was performed with methanol (Sangon Biotech; 2 mL/well). After aspirating the fixative, 2–3 mL of Giemsa staining solution (Sangon Biotech) was added per well. After staining for 2 h, blue colonies containing > 50 cells were counted in each well.

Flow cytometry

Cells in the shCtrl and shTastin groups were collected 72 h after infection with lentiviruses. Flow cytometry was performed routinely (Supplementary Material). The data were analyzed with the Modfit LT V5.0 software for cell cycle distribution.

Wound-healing assay

A 12-well plate was used for plating. When the tumor cell confluence reached 80–90%, the medium was aspirated, and low-serum medium was added. A 10-μL pipette tip was used to make a line on the monolayer. The dish underwent two phosphate-buffered saline (PBS) washes, and imaging was performed under a microscope (Leica). The dish was then placed in an incubator. The dish was photographed at 12 and 24 h. The ImageJ software was used to calculate tumor cell migration distance and rate.

Transwell assay

The Transwell assay was used for determining cell invasion (Supplementary Material).

Xenograft mouse model

Animals were purchased from GemPharmatech (Nanjing, China) and housed in a certified facility. Experiments involving animals had approval from the Institutional Animal Care and Use Committee (IACUC) of Anhui Medical University, following Association for Assessment and Accreditation of Laboratory Animal Care (AAALAC) guidelines. Two groups (shCtrl and shTastin, $n = 9$/each group) were established using A549 cells infected with shCtrl and shTastin, respectively. After one week of adaptive feeding with *ad libitum* chow and water, the animals underwent subcutaneous inoculation with negative virus-infected A549 cells or tastin shRNA virus-infected A549 cells (10^6 cells/mouse) in the right axilla. After 7–10 days, most nude mice developed tumors of 5 mm in their right axilla. This was recorded as Day 0, and tumor volume measurement was started. (1) The longest diameter of the tumor and (2) the diameter perpendicular to the longest diameter were measured using Vernier Calipers, and tumor volume was derived as $(\pi/6)\ ab^2$. Tumor volumes were determined at three-day intervals, and experiments were terminated on Day 18. Animals were anesthetized intraperitoneally with 0.7% pentobarbital and photographed. After euthanasia, tumor tissues were removed using surgical instruments and weighed and photographed. The relative tumor volume (RTV) was calculated as the ratio of the measured tumor volume for each animal to the tumor volume of the same animal at Day 0 (Table 2). The growth curve of the transplanted tumors was plotted for each group of animals and fitted using the Gompertz model $y = e^{b(1-e^{-ax})}$ (y is RTV, x is time, and a and b are parameters) and the Origin software. Tumor growth time and tumor growth retardation time were calculated according to the Gompertz model. Tumor growth time (TGT5) was the number of days until RTV increased by five times. Tumor growth retardation time (TGD) was the difference in tumor growth time between the shTastin and shCtrl groups. The inhibition rates of the transplanted tumors were calculated based on tumor weight volume at the time of euthanasia. The graft tumor suppression rate was 1 minus tumor weight in the shTastin group divided by tumor weight in the shCtrl group. The animals were sacrificed by CO_2 asphyxiation, and the tumors were excised and weighed. Sections underwent hematoxylin and eosin staining and immunohistochemistry for Ki67 detection. Assays involving animals followed the National Institutes of Health Guide for the Care and Use of Laboratory Animals.

Ethical approval

In total, 30 lung adenocarcinoma and 25 lung squamous cell carcinoma cases treated from December 2018 to June 2019 in the Pathology Department of the First Affiliated Hospital of Anhui Medical University were included. Patients with a history of other types of tumors or obvious organ dysfunction were excluded. The study had approval from the Institutional Review Board of Anhui Medical University (No. PJ2018-16-15). Each patient provided signed informed consent.

Statistical analysis

Microsoft Excel and GraphPad Prism were used for data analysis. Comparisons were carried out by the Student's *t*-test, with $P < 0.05$ indicating statistical significance.

Table 1. The expression of tastin in lung cancer and normal lung tissues.

Dataset No.	Title	Release time	Experimental design and samples	Pulmonary adenocarcinoma compared with normal tissues, tastin expression increased fold	Corrected *P* value (Benjamini and Hochberg FDR method)
GSE81089	Next-generation sequencing (RNAseq) of NSCLC	2016.6	108 cases of lung adenocarcinoma, 67 cases of lung squamous cell carcinoma, 24 cases of large cell carcinoma, 19 cases of normal lung tissue	6.06 ± 0.12	4.34×10^{-12}
GSE74706	Transcriptome of human NSCLC tissues	2016.5	Paired design, 10 pairs of lung adenocarcinoma and adjacent tissues, 8 pairs of lung squamous cell carcinoma and adjacent tissues	9.99 ± 0.41	4.86×10^{-5}
GSE40419	The transcriptional landscape and mutational profile of lung adenocarcinoma	2012.9	87 cases of lung adenocarcinoma, 77 cases of adjacent tissue	3.76 ± 0.09	5.17×10^{-33}
GSE19188	Expression data for early-stage NSCLC	2010.5	45 cases of lung adenocarcinoma, 27 cases of lung squamous cell carcinoma, 19 cases of large cell carcinoma, 65 cases of normal lung tissue	2.95 ± 0.06	3.12×10^{-20}

NSCLC: non-small-cell lung cancer; FDR: false discovery rate.

Table 2. Tumor volume of A549 cell transplanted tumor model in nude mice (mm^3).

Group	Day 0	Day 3	Day 6	Day 9	Day 12	Day 15	Day 18
shCtrl	111.019 ± 12.885	144.763 ± 18.206	180.565 ± 25.064	213.464 ± 28.501	267.463 ± 40.755	332.148 ± 50.478	440.447 ± 66.258
shTastin	63.162 ± 11.959	74.323 ± 11.195	82.769 ± 14.906	92.194 ± 15.371	102.765 ± 18.871	116.316 ± 27.542	127.378 ± 30.903

Results

Tastin is upregulated in NSCLC

To profile tastin expression in tumor tissues, we analyzed multiple sets of RNAseq data in the GEO database. Tastin expression levels were markedly elevated in lung adenocarcinoma in comparison with non-cancerous lung tissue (Table 1). Immunohistochemistry showed high tastin expression in lung adenocarcinoma and squamous cell carcinoma tissue specimens, mainly distributed in the cytoplasm (Figure 1(A)). Tastin amounts were lower in adjacent tissue specimens compared with tumor tissue specimens (Figure 1(A)). We next calculated H-scores in 30 lung adenocarcinoma patients and 25 pairs of lung squamous cell carcinoma tissues after immunohistochemistry. Tastin expression was significantly higher in lung adenocarcinoma and squamous cell carcinoma tissue specimens in comparison with non-cancerous specimens, suggesting tastin might be related to the pathogenesis of lung tumors. Of the 30 pairs of lung adenocarcinoma samples, H-scores for tastin were higher in tumor tissue specimens in comparison with adjacent tissue samples in 23 pairs, accounting for 92.0%, including 11 (36.7%) that showed more than twofold upregulation (Figure 1(B)). Of the 25 pairs of lung squamous cell carcinoma samples, H-scores for tastin were also higher in tumor tissue specimens, with 9 pairs (36.0%) showing significant differences (Figure 1(C)). In agreement, tastin expression was markedly elevated in lung cancer in comparison with non-cancerous tissue specimens (Figure 2(A)). Furthermore, KM analysis revealed that among lung adenocarcinoma cases, median survival times were 41.2 and 54.2 months in the high- and low-tastin expression groups, respectively (Figure 2(B)), with statistical significance ($P = 0.004$, log-rank test statistics = 8.181). This suggested high tastin expression cases showed reduced survival time and a poor prognosis.

Tastin enhances NSCLC cell proliferation

We next examined tastin's role in NSCLC cells. A549 (human lung adenocarcinoma) and NCI-H226 (squamous cell carcinoma) cells were used to examine the role of tastin in cell proliferation by knocking down tastin (Figure 3(A) and (B)). In MTT assays, lung adenocarcinoma cells had markedly lower Optical Density (OD) values after tastin silencing compared with the control group (Figure 3(C)). In human lung squamous cells, similar findings were obtained (Figure 3(D)). The above results indicated that knockdown of the tastin gene decreased the proliferative ability of NSCLC cells. The tastin knockdown groups yielded significantly lower numbers of colonies than the control groups of A549 and NCI-H226 cells. Moreover, quantitative analysis showed an increased number of colonies formed after overexpressing the tastin gene. This indicated tastin exerted an inhibitory effect on the colony formation ability of human NSCLC cells (Figure 3(E)). In cell cycle distribution analysis, A549 cell amounts in G1 were increased after tastin knockdown, while

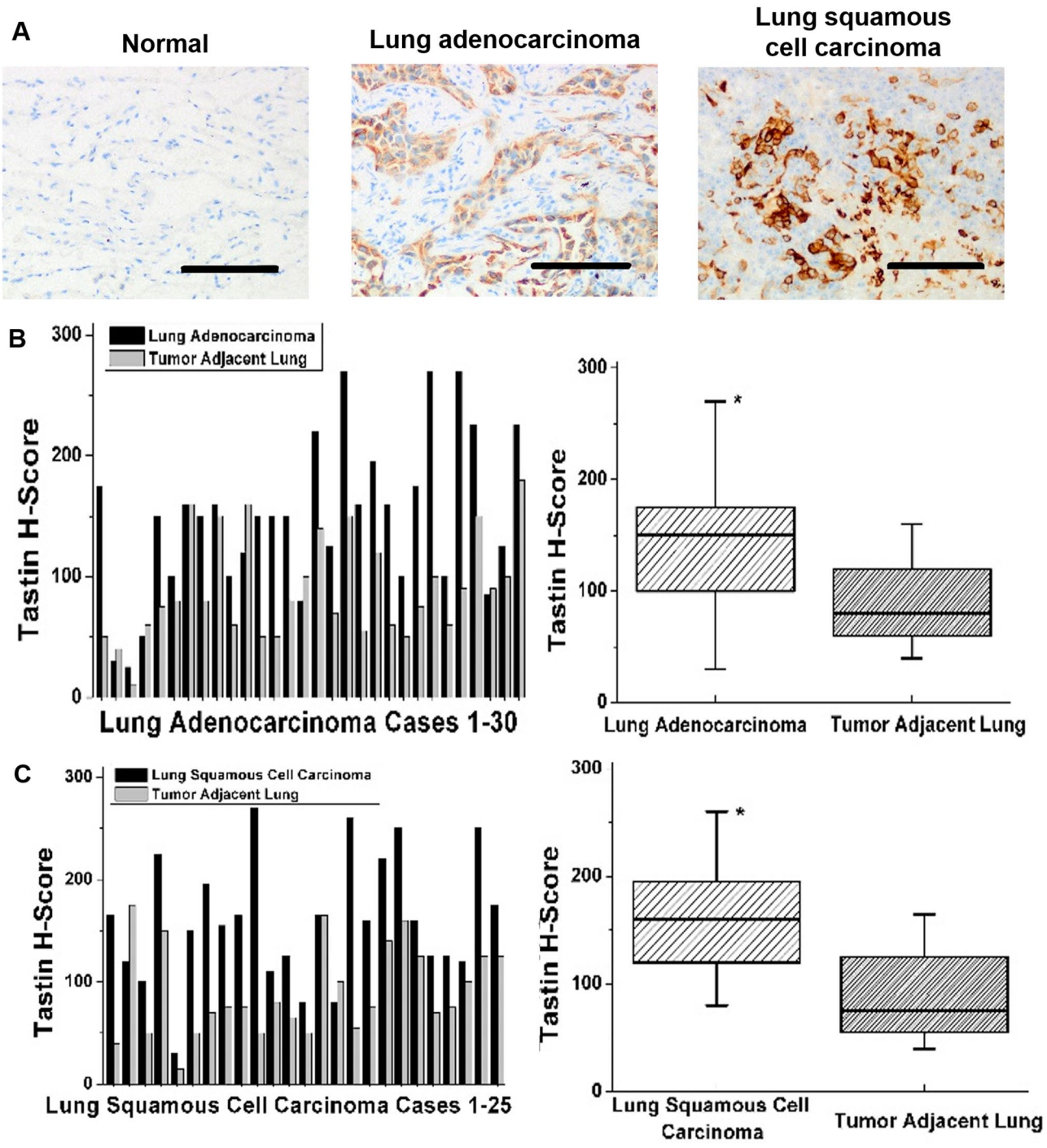

Figure 1. Tastin is upregulated in NSCLC. (A) Immunohistochemistry showing tastin expression in non-cancerous lung (left), lung adenocarcinoma (middle), and lung squamous cell carcinoma (right) tissue specimens. Scale bar: 400 μm. (B) Tastin H-scores in 30 pairs were markedly increased in lung adenocarcinoma compared with adjacent tissues. *$P < 0.05$. (C) Tastin H-scores in 25 pairs were increased in lung squamous cell carcinoma compared with adjacent tissue samples. *$P < 0.05$.

G2/M phase cells were markedly decreased (Figure 4(A)); however, there was no significant difference in S-phase cell amounts. The proportion of squamous cell carcinoma cells in G1 was also elevated, while that of S-phase cells were starkly lower (Figure 4(B)). There was no significant difference in G2/M phase cell rates. These results showed that in NSCLC cells with tastin silencing, cell cycle distribution is altered, with induced G1 arrest.

Tastin promotes NSCLC cell invasion and migration

Next, we examined whether the migratory ability of NSCLC cells would be regulated by tastin. In the wound-healing assay, tastin knockdown impaired migration in lung cancer cells. The migration rates in the tastin knockdown groups were markedly reduced in comparison with respective control groups of A549 cells at 12 and 24 h after scratching

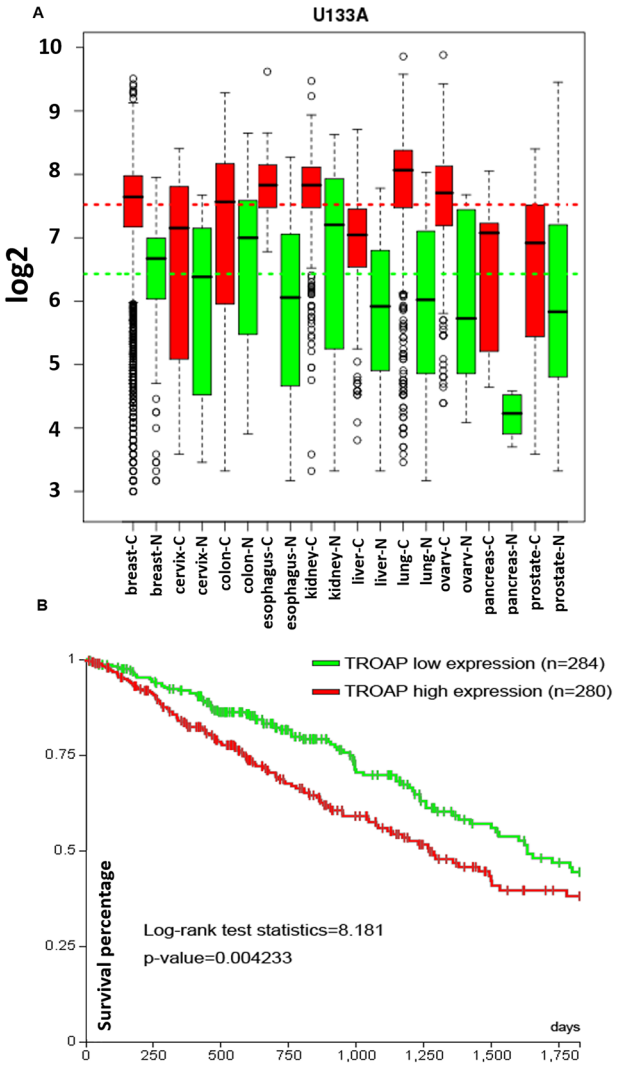

Figure 2. Tastin expression in various tumors and its impact on survival. (A) Tastin expression in a variety of tumors and corresponding normal tissues. C: Red, N: Normal. (B) The association of tastin abundance with patient survival in lung adenocarcinoma was assessed by the KM method. *$P=0.05$ versus 8.181%. TROAP low expression ($n=284$); TROAP high expression ($n=280$).

(Figure 5(A)). In NCI-H226 cells, migration rates after tastin silencing were also significantly decreased in comparison with control cells (Figure 5(B)). The above findings suggested tastin might control the migratory ability of NSCLCs. We then examined the invasive ability of NSCLC cells after tastin silencing. The average numbers of A549 and NCI-H226 cells invading the chamber per field of view were significantly reduced in tastin knockdown cells compared with controls (Figure 5(C) and (D)). The above findings suggested decreased invasion in human lung cancer adenocarcinoma and squamous cell carcinoma cells after tastin silencing.

Tastin regulates PI3K/AKT and ERK1/2 signaling via ErbB4

To determine the downstream pathways that mediate the function of tastin in NSCLC cells, we screened the potential proteins interacting with tastin in STRING 10.0 (http://version10.string-db.org/) and tastin was predicted to interact with ErbB4 (Supplementary Figure S1). Therefore, we detected whether pathways downstream of the EGFR pathway would be affected by tastin. After tastin silencing in A549 and NCI-H226 cells, phosphorylated ERK and AKT levels were decreased, indicating downregulated Ras/Raf/MEK/ERK signaling and suggesting that the PI3K/AKT pathway was activated by tastin (Figure 6(A) to (D)). In addition, epithelial–mesenchymal transition (EMT) biomarkers were examined. As a result, N-cadherin and vimentin (mesenchymal markers) were decreased after tastin knockdown, while E-cadherin (epithelial marker) was increased, suggesting that tastin might affect cell adhesion protein expression and thus participate in tumor cell invasion and migration (Figure 6(A)). These findings suggested tastin may induce MEK/ERK and PI3K/AKT pathway activation and participate in tumor cell invasion and migration.

Tastin promotes NSCLC growth in the mouse xenograft model

Then, we verified the effect of tastin on NSCLC cell growth in mice. To this end, nude mice were inoculated with control or tastin knockdown NSCLC cells subcutaneously. With time, tumor volumes in both groups increased. As expected, the volumes of the transplanted tumors were starkly larger in the control group compared with the tastin knockdown group (Figure 7(A) and (B)). Besides, the average weights of the transplanted tumors were smaller in the tastin knockdown group than control animals (Figure 7(C) and (D)). Figure 7(E) shows H&E staining and Ki67 analysis of the xenograft tumors; Ki67 expression appeared to be decreased in the tastin knockdown group. Taken together, the growth rate of A549 tumors was remarkably reduced after tastin silencing compared with control animals, suggesting tastin promoted NSCLC growth in the mouse xenograft model.

Clinical significance of tastin in lung adenocarcinoma

Next, the clinical relevance of tastin was examined by analyzing 30 lung adenocarcinoma cases and 25 lung squamous cell carcinoma specimens. H-scores for tastin were significantly elevated in cases at a later NSCLC stage (Stages III–IV) compared with those at an earlier stage (Stages I–II). H-scores were significantly elevated in patients with distant metastasis (M1) compared with those without distant metastasis (M0) (Tables 3 and 4). Patients with high expression of the cell proliferation-related protein Ki-67 ($\geqslant$15%) showed starkly higher tastin levels compared with the low Ki-67 expression group ($<$15%) (Tables 3 and 4).

Discussion

It was previously shown that elevated tastin (TROAP) independently predicts poor prognosis in liver cancer, based on overall survival data.[15] Li *et al.* also revealed that

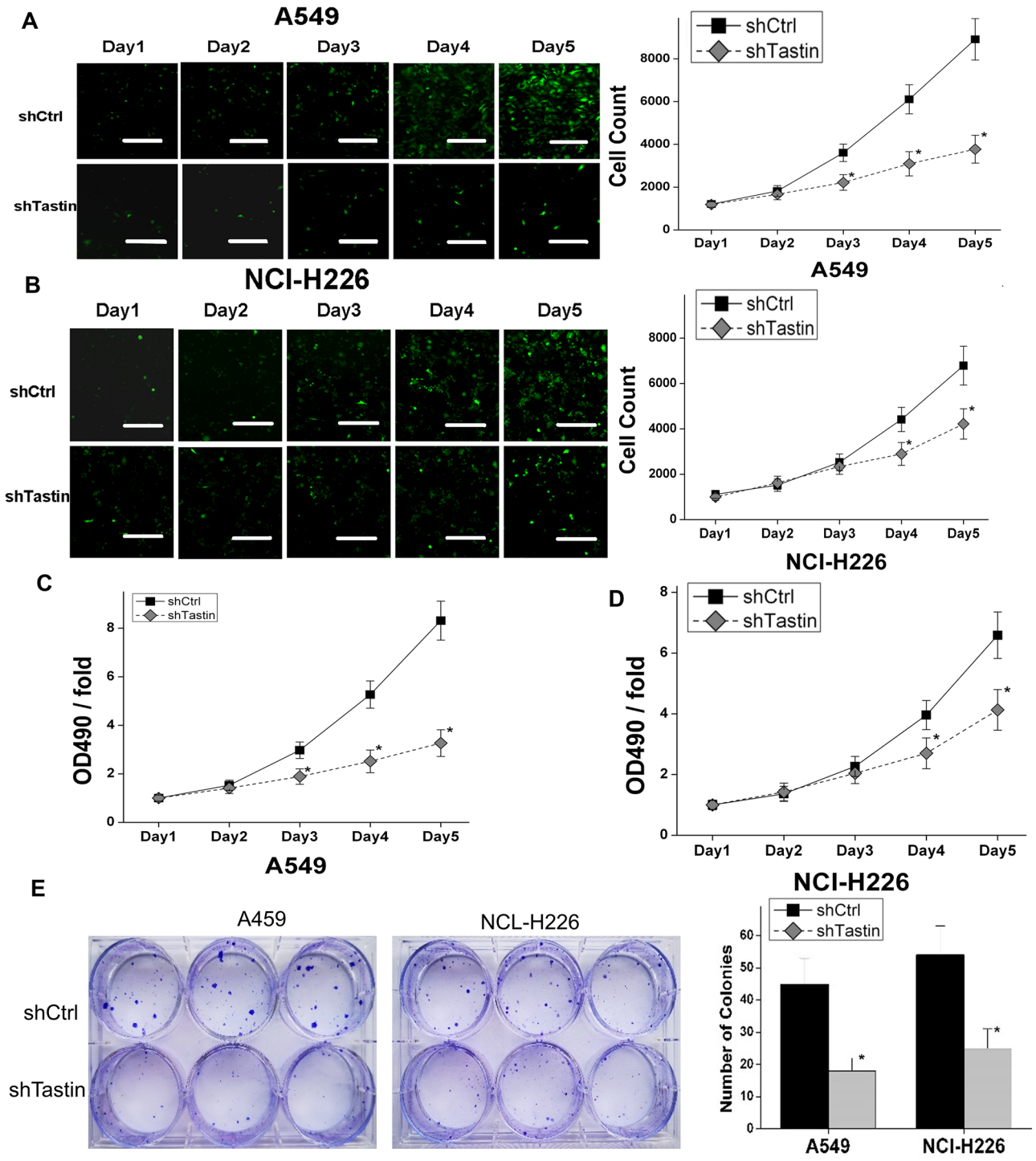

Figure 3. Tastin promotes NSCLC cell proliferation. (A) Tastin was knocked down in A549 cells, which were compared to controls. Cell proliferation was analyzed on a Celigo automatic cell counting analyzer. *$P < 0.05$. Scale bar: 400 μm. (B) Tastin was knocked down in NCI-H226 cells, which were compared to controls. Cell proliferation was analyzed on a Celigo automatic cell counting analyzer. *$P < 0.05$. Scale bar: 400 μm. (C) The viability of A549 cells after tastin knockdown compared to control cells was analyzed by the MTT assay. *$P < 0.05$. (D) The viability of NCI-H226 cells after tastin knockdown compared to control cells was analyzed by the MTT assay. *$P < 0.05$. (E) Detection of colony formation ability in A549 and NCI-H226 cells after tastin knockdown compared to control cells. *$P < 0.05$.

tastin promotes breast cancer proliferation and metastasis. In cell culture assays, tastin silencing markedly reduced breast cancer cell proliferation and G1 to S progression, and migratory and invasive capabilities. The study indicated that tastin is essential in enhancing malignancy in breast cancer cells.[26] In this study, tastin knockdown resulted in decreased EMT, reflected by E-cadherin, N-cadherin, and vimentin expression. In addition, a report applying multiple data fusion analyses demonstrated elevated tastin amounts are correlated with shorter survival in glioma

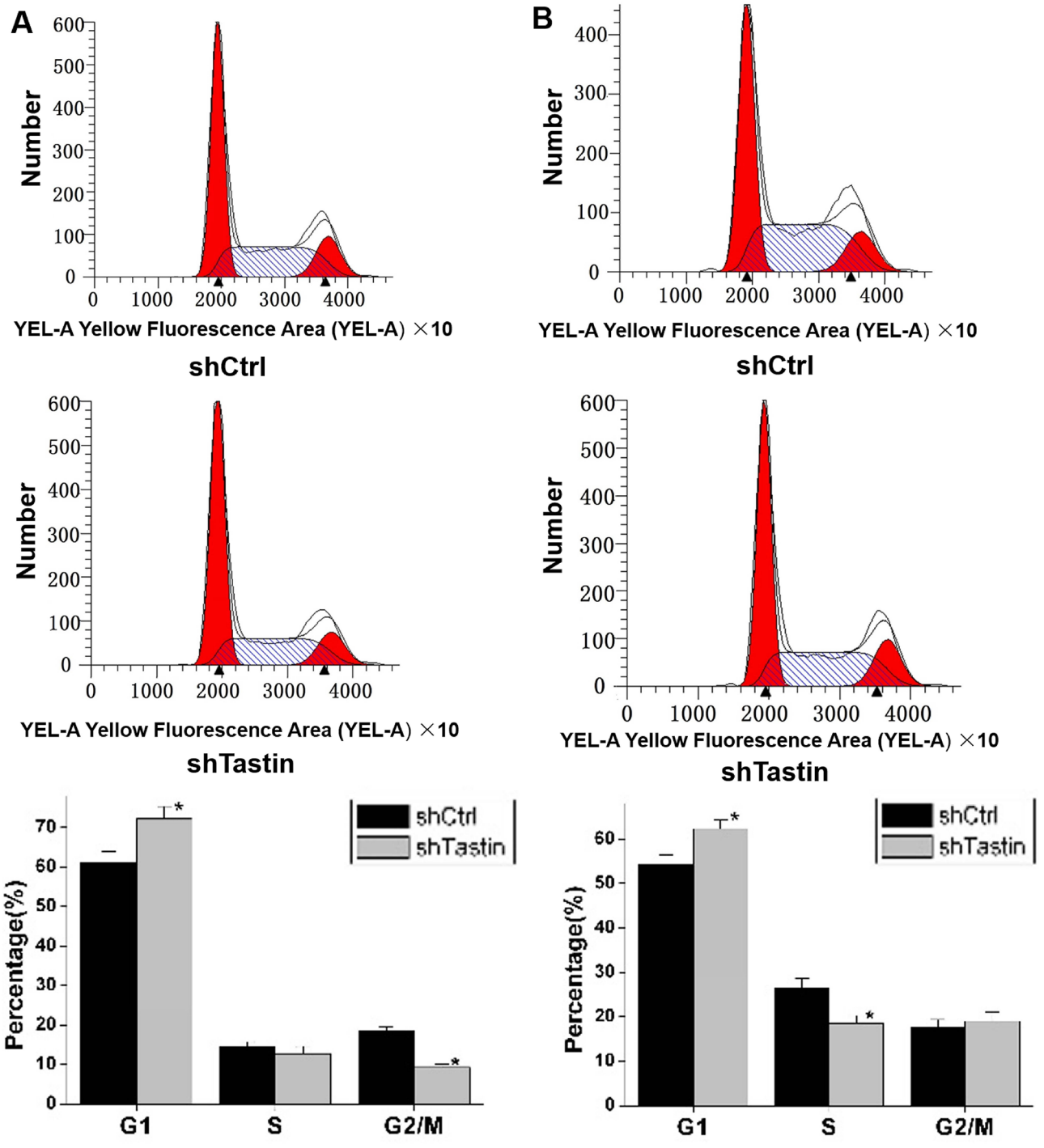

Figure 4. Impact of tastin on the cell cycle. (A) Cell cycle distribution of A549 cells after tastin knockdown compared to control cells analyzed flow cytometrically. *$P < 0.05$. (B) Cell cycle distribution of NCI-H226 cells after tastin knockdown compared to control cells analyzed flow cytometrically. *$P < 0.05$.

cases.[27] Moreover, tastin expression was suggested to independently predict prognosis in lung adenocarcinoma cases in a study by Chen and colleagues.[28] As shown above, tastin levels were elevated in tumor samples, especially NSCLC, and increased tastin expression was associated with poorer patient prognosis. Therefore, we first speculated and confirmed that tastin plays a promoting role in NSCLC occurrence and progression. We demonstrated that tastin deficiency indeed impaired the growth rate and viability of NSCLC cells and impeded NSCLC cell metastasis, consistent with our hypothesis.

ErbB4 represents an EGFR family member with tyrosine kinase activity. Meanwhile, tastin is predicted to have many potential phosphorylation sites and can be phosphorylated after binding to ErbB4.[18,29–33] This study also demonstrated that tastin interacted with ErbB4 and inhibited NSCLC cells

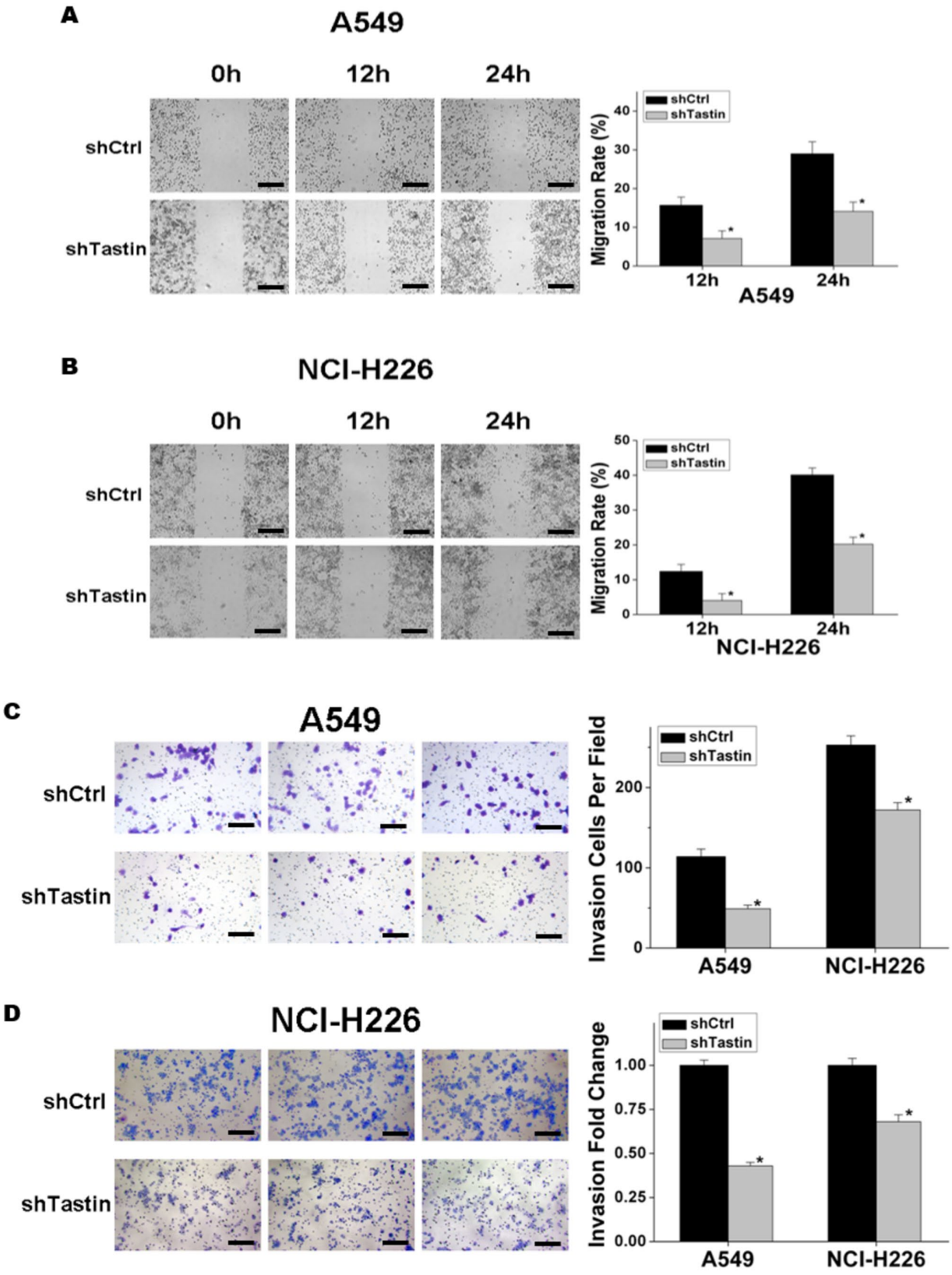

Figure 5. Tastin promotes NSCLC cell metastasis. (A) Migratory ability of A549 cells after tastin knockdown compared to control cells analyzed by the wound-healing assay. *$P < 0.05$. Scale bar: 200 μm. (B) Migratory ability of NCI-H226 cells after tastin knockdown compared to control cells analyzed by the wound-healing assay. *$P < 0.05$. Scale bar: 200 μm. (C) Invasive ability of A549 cells after tastin knockdown compared to control cells analyzed by the Transwell invasion assay. *$P < 0.05$. Scale bar: 50 μm. (D) Invasive ability of NCI-H226 cells after tastin knockdown compared to control cells analyzed by the Transwell invasion assay. * $P < 0.05$. Scale bar: 50 μm.

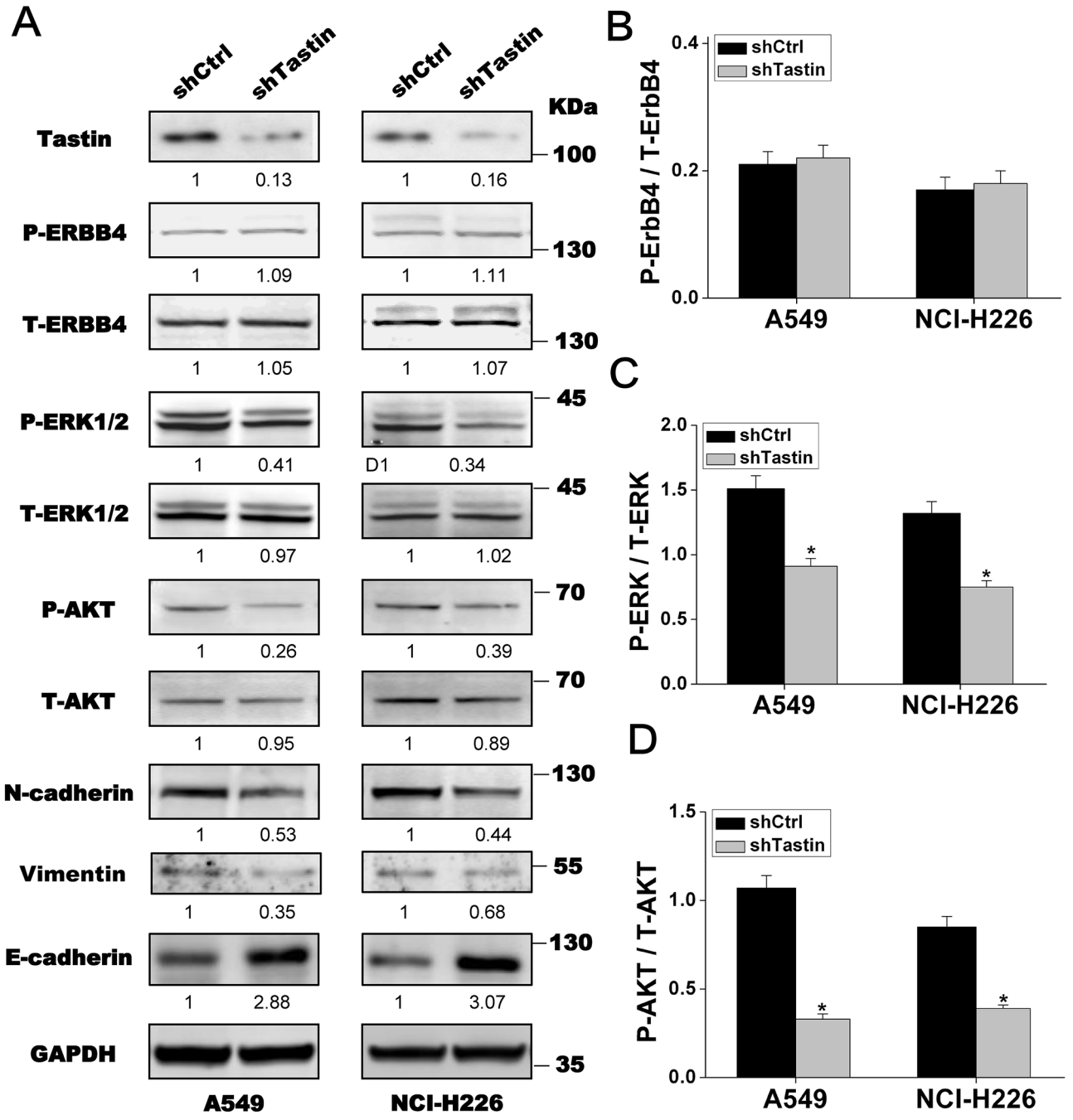

Figure 6. Tastin activates the ERK and AKT pathways via ErbB4. (A) Western blot analysis of A549 and NCI-H226 cells after tastin knockdown compared to controls (ref = 1.00). (B) Quantitative analysis of P-ErbB4 and T-ErbB4 levels after tastin knockdown compared to controls in A549 and NCI-H226 cells. (C) Quantitative analysis of P-ERK1/2 and T-ERK1/2 levels after tastin knockdown compared to controls in A549 and NCI-H226 cells. *$P < 0.05$. (D) Quantitative analysis of P-AKT and T-AKT levels after tastin knockdown compared to controls in A549 and NCI-H226 cells. *$P < 0.05$.

in knockdown experiments. A report by Sugihara and collaborators also showed tastin interacted with ErbB4, which somewhat resembles tastin and ErbB4 interaction found in this study. Sugihara *et al.*[34] revealed interactions of TRO, bystin, and ErbB4, which were observed by Western blot analysis of target proteins in HT-H cells on transfection with individual siRNAs. Moreover, TROAP regulates prostate cancer progression through WNT3/survivin signaling,[35] regulates the cell cycle, and promotes tumor progression via Wnt/β-catenin signaling in glioma.[36] It was also found by Li and colleagues[26] that TROAP induces malignancy in breast cancer cells via TROAP silencing. Meanwhile, reduced TROAP amounts suppress malignancy, as reported in gastric cancer.[16] These studies indicate that ErbB4-Ras-Raf-MEK-ERK or ErbB4-PI3K-AKT pathway activation might control tastin-related induction NSCLC progression. Nevertheless, total and phosphorylated ErbB4 amounts were not regulated by tastin. One possible explanation is

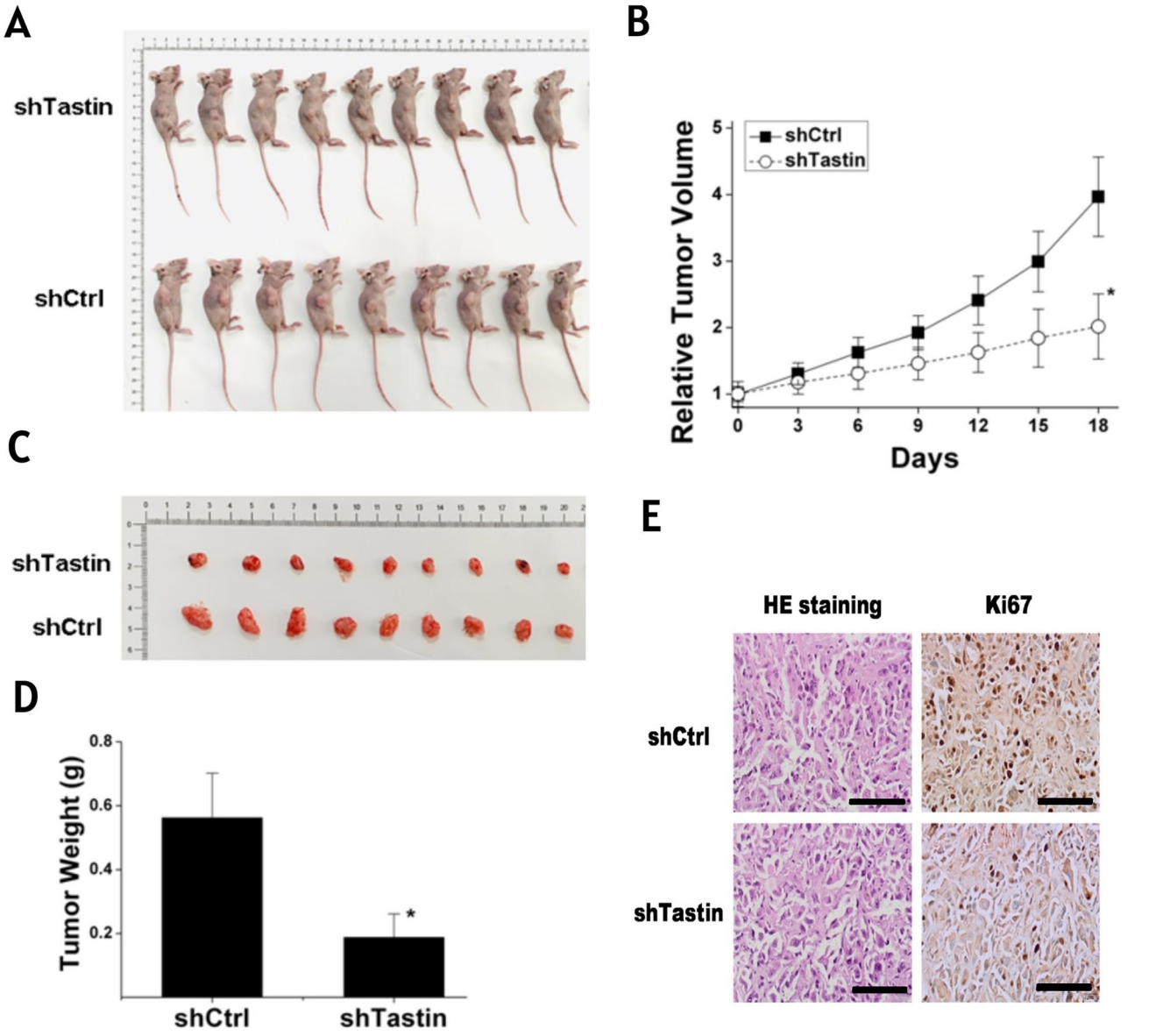

Figure 7. Tastin promotes tumor growth in the mouse xenograft model. (A) Photographs of mice with xenografts taken 18 days after injection in the control and tastin knockdown groups. (B) RTVs of xenografts after tastin knockdown versus control animals. *$P < 0.05$. (C) Photographs of xenografts extracted from mice in the control and tastin knockdown groups. (D) Weights of xenografts harvested 18 days after injection in the tastin knockdown and control groups. *$P < 0.05$. (E) H&E staining and Ki67 examinations of xenograft tumors in the tastin knockdown and control groups. Scale bar: 200 μm.

that tastin might function as an adapter to facilitate interactions with ErbB4 and its downstream factors, but confirmation is required.

Furthermore, the Bcl2 family of proteins is considered major factors controlling apoptosis. The mechanism of Bcl2 proteins and their effects in multiple pathologies are well known.[37] A previous study indicated that Bcl2 inhibitors have the potential to treat solid tumors.[38] Moreover, Mirakhor *et al.*[39] revealed that Bcl2/Bax is markedly upregulated in the malignancy group and a loss of Bax expression in endometrial carcinoma was reported.[40] This study also found that Bcl2 and Bax were downregulated and upregulated, respectively, after transfection with tastin shRNA (Supplementary Figure S3). This suggests that there might be other mechanisms, including apoptosis mediating the role of tastin in NSCLC. Therefore, an ongoing study in our laboratory explores the mechanisms (including apoptosis and the ERBB4 axis) of tastin in cancer in-depth, using a full array of shRNAs.

In conclusion, higher tastin expression appears to be associated with faster growth rate, later stage, and metastasis in NSCLC. This suggests that tastin might be a potential biomarker of NSCLC development. These findings highlight tastin's role in NSCLC occurrence and progression and provide a potential target for developing a new treatment option for NSCLC (Supplementary Figure S2).

Table 3. The clinical relevance of tastin in lung adenocarcinoma cases.

Clinicopathological characteristics	*n*	Tastin H-score Median (P25, P75)	*P* value
Gender			0.188
Male	14	152.50 (95.00, 172.50)	
Female	11	165.00 (125.00, 225.00)	
Age (years)			0.156
⩾60	10	170.00 (123.75, 231.25)	
<60	15	150.00 (100.00, 165.00)	
T staging			0.107
T_1–T_2	15	150.00 (120.00, 165.00)	
T_3–T_4	10	197.50 (113.75, 250.00)	
N staging			0.227
N_0	11	155.00 (120.00, 165.00)	
N_1–N_3	14	170.00 (118.75, 250.00)	
M staging			0.037
M_0	15	150.00 (120.00, 165.00)	
M_1	10	210.00 (118.75, 252.50)	
Total staging			0.107
I–II	10	152.50 (117.50, 161.25)	
III–IV	15	175.00 (125.00, 250.00)	
Ki-67 (%)			0.020
<15	6	115.00 (67.50, 146.25)	
⩾15	12	180.00 (157.50, 250.00)	
Smoking history			0.395
Yes	9	150.00 (80.00, 222.50)	
No	16	162.50 (125.00, 208.75)	
Pleural fluid			0.059
No	22	152.50 (117.50, 172.50)	
Yes	3	225.00 (200.00, 237.50)	
EGFR status			0.180
Mutant	1	110.00	
Wild type	3	165.00 (145.00, 207.50)	

EGFR: epidermal growth factor receptor.

Table 4. The clinical relevance of Tastin lung squamous cell carcinoma cases.

Clinicopathological characteristics	*n*	Tastin H-score Median (P25, P75)	*Z* value	*P* value
Gender			–0.606	0.545
Male	14	150.00 (100.00, 175.00)		
Female	16	155.00 (106.25, 213.75)		
Age (years)			–1.447	0.148
⩾60	12	110.00 (88.75, 171.25)		
<60	18	155.00 (125.00, 221.25)		
T staging			–1.017	0.309
T_1–T_2	20	150.00 (100.00, 160.00)		
T_3–T_4	10	172.50 (115.00, 225.00)		
N staging			–1.565	0.118
N_0	13	150.00 (75.00, 160.00)		
N_1–N_3	16	155.00 (106.25, 225.00)		
M staging			–2.152	0.031
M_0	16	150.00 (85.00, 157.50)		
M_1	14	167.50 (118.75, 236.25)		
Total staging			–2.064	0.039
I–II	12	135.00 (62.5, 157.5)		
III–IV	18	160 (118.75, 225.00)		
Ki-67 (%)			–2.728	0.006
<15	8	100.00 (43.75, 115.00)		
⩾15	13	175.00 (150.00, 247.50)		
Smoking history			–0.789	0.430
No	7	120.00 (100.00, 160.00)		
Yes	23	150.00 (100.00, 195.00)		
Pleural fluid			–1.846	0.065
No	25	150.00 (100.00, 167.50)		
Yes	5	195.00 (142.50, 247.50)		
EGFR status			–1.065	0.287
Mutant	10	150.00 (96.25, 202.50)		
Wild type	v4	190.00 (133.75, 257.50)		

EGFR: epidermal growth factor receptor.

AUTHORS' CONTRIBUTIONS

YL conceived and designed the project. AY and MC carried out experiments and data analysis. YZ, WW, LF, FW, FZ, and HY provided technical assistance. YL and YLu drafted the manuscript.

DECLARATION OF CONFLICTING INTERESTS

The author(s) declared no potential conflicts of interest with respect to the research, authorship, and/or publication of this article.

ETHICAL APPROVAL

The study had approval from the Institutional Review Board of Anhui Medical University (No. PJ2018-16-15), following the 1964 Declaration of Helsinki and its subsequent amendments. Each patient provided signed informed consent.

FUNDING

The author(s) disclosed receipt of the following financial support for the research, authorship, and/or publication of this article: The present project was funded by the Provincial Natural Science Foundation of Anhui (1808085QH232) and the Youth Development Program of the First Affiliated Hospital of Anhui Medical University (2018kj33).

ORCID ID

Yu Lei https://orcid.org/0000-0003-2055-8194

SUPPLEMENTAL MATERIAL

Supplemental material for this article is available online.

REFERENCES

1. Cardona AF, Ricaurte L, Zatarain-Barrón ZL, Arrieta O. Squamous cell lung cancer: genomic evolution and personalized therapy. *Salud Publica Mex* 2019;**61**:329–38
2. Yuan M, Huang LL, Chen JH, Wu J, Xu Q. The emerging treatment landscape of targeted therapy in non-small-cell lung cancer. *Signal Transduct Target Ther* 2019;**4**:61
3. Chen R, Manochakian R, James L, Azzouqa AG, Shi H, Zhang Y, Zhao Y, Zhou K, Lou Y. Emerging therapeutic agents for advanced non-small cell lung cancer. *J Hematol Oncol* 2020;**13**:58
4. Hu H, Xu L, Chen Y, Luo SJ, Wu YZ, Xu SH, Liu MT, Lin F, Mei Y, Yang Q, Qiang YY, Lin YW, Deng YJ, Lin T, Sha YQ, Huang BJ, Zhang SJ. The upregulation of trophinin-associated protein (TROAP) predicts a poor prognosis in hepatocellular carcinoma. *J Cancer* 2019;**10**:957–67
5. Santos LL, Ling CK, Dimitriadis E. Tripeptidyl peptidase I promotes human endometrial epithelial cell adhesive capacity implying a role in receptivity. *Reprod Biol Endocrinol* 2020;**18**:124
6. Rawlings TM, Makwana K, Taylor DM, Molè MA, Fishwick KJ, Tryfonos M, Odendaal J, Hawkes A, Zernicka-Goetz M, Hartshorne GM, Brosens JJ, Lucas ES. Modelling the impact of decidual senescence

on embryo implantation in human endometrial assembloids. *eLife* 2021;**10**:69603
7. Yoshihara M, Mizutani S, Kato Y, Matsumoto K, Mizutani E, Mizutani H, Fujimoto H, Osuka S, Kajiyama H. Recent insights into human endometrial peptidases in blastocyst implantation via shedding of microvesicles. *Int J Mol Sci* 2021;**22**:13479
8. Godoy H, Mhawech-Fauceglia P, Beck A, Miliotto A, Miller A, Lele S, Odunsi K. Developmentally restricted differentiation antigens are targets for immunotherapy in epithelial ovarian carcinoma. *Int J Gynecol Pathol* 2013;**32**:536–40
9. Fukuda MN, Sugihara K. Trophinin in cell adhesion and signal transduction. *Front Biosci (Elite Ed)* 2012;**4**:342–50
10. Park SK, Yoon J, Wang L, Shibata TK, Motamedchaboki K, Shim KJ, Chang MS, Lee SH, Tamura N, Hatakeyama S, Nadano D, Sugihara K, Fukuda MN. Enhancement of mouse sperm motility by trophinin-binding peptide. *Reprod Biol Endocrinol* 2012;**10**:101
11. Rawla P. Epidemiology of prostate cancer. *World J Oncol* 2019;**10**:63–89
12. Ayala GE, Dai H, Li R, Ittmann M, Thompson TC, Rowley D, Wheeler TM. Bystin in perineural invasion of prostate cancer. *Prostate* 2006;**66**:266–72
13. Jin L, Zhou Y, Chen G, Dai G, Fu K, Yang D, Zhu J. EZH2-TROAP pathway promotes prostate cancer progression via TWIST signals. *Front Oncol* 2020;**10**:592239
14. Li L, Wei JR, Song Y, Fang S, Du Y, Li Z, Zeng TT, Zhu YH, Li Y, Guan XY. TROAP switches DYRK1 activity to drive hepatocellular carcinoma progression. *Cell Death Dis* 2021;**12**:125
15. Jiao Y, Li Y, Lu Z, Liu Y. High trophinin-associated protein expression is an independent predictor of poor survival in liver cancer. *Dig Dis Sci* 2019;**64**:137–43
16. Jing K, Mao Q, Ma P. Decreased expression of TROAP suppresses cellular proliferation, migration and invasion in gastric cancer. *Mol Med Rep* 2018;**18**:3020–6
17. Fujiwara H, Ono M, Sato Y, Imakawa K, Iizuka T, Kagami K, Fujiwara T, Horie A, Tani H, Hattori A, Daikoku T, Araki Y. Promoting roles of embryonic signals in embryo implantation and placentation in cooperation with endocrine and immune systems. *Int J Mol Sci* 2020;**21**:1885
18. El-Gamal MI, Mewafi NH, Abdelmotteleb NE, Emara MA, Tarazi H, Sbenati RM, Madkour MM, Zaraei SO, Shahin AI, Anbar HS. A review of HER4 (ErbB4) kinase, its impact on cancer, and its inhibitors. *Molecules* 2021;**26**:7376
19. Xu B, Huo Z, Huang H, Ji W, Bian Z, Jiao J, Sun J, Shao J. The expression and prognostic value of the epidermal growth factor receptor family in glioma. *BMC Cancer* 2021;**21**:451
20. Moghbeli M, Makhdoumi Y, Soltani Delgosha M, Aarabi A, Dadkhah E, Memar B, Abdollahi A, Abbaszadegan MR. ErbB1 and ErbB3 co-over expression as a prognostic factor in gastric cancer. *Biol Res* 2019;**52**:2
21. Cao Z, Liao Q, Su M, Huang K, Jin J, Cao D. AKT and ERK dual inhibitors: the way forward? *Cancer Lett* 2019;**459**:30–40
22. Yu D, Hung MC. Overexpression of ErbB2 in cancer and ErbB2-targeting strategies. *Oncogene* 2000;**19**:6115–21
23. Hu X, Xu H, Xue Q, Wen R, Jiao W, Tian K. The role of ERBB4 mutations in the prognosis of advanced non-small cell lung cancer treated with immune checkpoint inhibitors. *Mol Med* 2021;**27**:126
24. Davis S, Meltzer PS. GEOquery: a bridge between the Gene Expression Omnibus (GEO) and BioConductor. *Bioinformatics* 2007;**23**:1846–7
25. Colaprico A, Silva TC, Olsen C, Garofano L, Cava C, Garolini D, Sabedot TS, Malta TM, Pagnotta SM, Castiglioni I, Ceccarelli M, Bontempi G, Noushmehr H. TCGAbiolinks: an R/Bioconductor package for integrative analysis of TCGA data. *Nucleic Acids Res* 2016;**44**:e71
26. Li K, Zhang R, Wei M, Zhao L, Wang Y, Feng X, Yang Y, Yang S, Zhang L. TROAP promotes breast cancer proliferation and metastasis. *Biomed Res Int* 2019;**2019**:6140951
27. Yong S, Zhen DL, Run ZL, Xiao YL, Xing BC, Yu LJ, Bin FL, Yan ZG, Xinjun W. Trophinin-associated protein expression correlates with shorter survival of patients with glioma: a study based on multiple data fusion analysis. *Mol Biol Rep* 2022;**49**:7899-909
28. Chen Z, Zhou Y, Luo R, Liu K, Chen Z. Trophinin-associated protein expression is an independent prognostic biomarker in lung adenocarcinoma. *J Thorac Dis* 2019;**11**:2043–50
29. Xu J, Gong L, Qian Z, Song G, Liu J. ERBB4 promotes the proliferation of gastric cancer cells via the PI3K/Akt signaling pathway. *Oncol Rep* 2018;**39**:2892–8
30. Arienti C, Pignatta S, Tesei A. Epidermal growth factor receptor family and its role in gastric cancer. *Front Oncol* 2019;**9**:1308
31. Elster N, Toomey S, Fan Y, Cremona M, Morgan C, Weiner Gorzel K, Bhreathnach U, Milewska M, Murphy M, Madden S, Naidoo J, Fay J, Kay E, Carr A, Kennedy S, Furney S, Mezynski J, Breathhnach O, Morris P, Grogan L, Hill A, Kennedy S, Crown J, Gallagher W, Hennessy B, Eustace A. Frequency, impact and a preclinical study of novel ERBB gene family mutations in HER2-positive breast cancer. *Ther Adv Med Oncol* 2018;**10**:1758835918778297
32. Liu S, Gong Y, Xu XD, Shen H, Gao S, Bao HD, Guo SB, Yu XF, Gong J. MicroRNA-936/ERBB4/Akt axis exhibits anticancer properties of gastric cancer through inhibition of cell proliferation, migration, and invasion. *Kaohsiung J Med Sci* 2021;**37**:111–20
33. Wang S, Li Z, Zhu G, Hong L, Hu C, Wang K, Cui K, Hao C. RNA-binding protein IGF2BP2 enhances circ_0000745 abundancy and promotes aggressiveness and stemness of ovarian cancer cells via the microRNA-3187-3p/ERBB4/PI3K/AKT axis. *J Ovarian Res* 2021;**14**:154
34. Sugihara K, Sugiyama D, Byrne J, Wolf DP, Lowitz KP, Kobayashi Y, Kabir-Salmani M, Nadano D, Aoki D, Nozawa S, Nakayama J, Mustelin T, Ruoslahti E, Yamaguchi N, Fukuda MN. Trophoblast cell activation by trophinin ligation is implicated in human embryo implantation. *Proc Natl Acad Sci USA* 2007;**104**:3799–804
35. Ye J, Chu C, Chen M, Shi Z, Gan S, Qu F, Pan X, Yang Q, Tian Y, Wang L, Yang W, Cui X. TROAP regulates prostate cancer progression via the WNT3/survivin signalling pathways. *Oncol Rep* 2019;**41**:1169–79
36. Zhao ZQ, Wu XJ, Cheng YH, Zhou YF, Ma XM, Zhang J, Heng XY, Feng F. TROAP regulates cell cycle and promotes tumor progression through Wnt/β-Catenin signaling pathway in glioma cells. *CNS Neurosci Ther* 2021;**27**:1064–76
37. Siddiqui WA, Ahad A, Ahsan H. The mystery of BCL2 family: Bcl-2 proteins and apoptosis: an update. *Arch Toxicol* 2015;**89**:289–317
38. Vogler M. Targeting BCL2-proteins for the treatment of solid tumours. *Adv Med* 2014;**2014**:943648
39. Mirakhor Samani S, Ezazi Bojnordi T, Zarghampour M, Merat S, Fouladi DF. Expression of p53, Bcl-2 and Bax in endometrial carcinoma, endometrial hyperplasia and normal endometrium: a histopathological study. *J Obstet Gynaecol* 2018;**38**:999–1004
40. Sakuragi N, Salah-eldin AE, Watari H, Itoh T, Inoue S, Moriuchi T, Fujimoto S. Bax, Bcl-2, and p53 expression in endometrial cancer. *Gynecol Oncol* 2002;**86**:288–96

(Received June 28, 2022, Accepted December 7, 2022)